universe

MDPI

Review

Topological Aspects of Dense Matter: Lattice Studies

Maria Paola Lombardo

Istituto Nazionale di Fisica Nucleare, Sezione di Firenze, 50019 Sesto Fiorentino, FI, Italy; lombardo@fi.infn.it

Abstract: Topological fluctuations change their nature in the different phases of strong interactions, and the interrelation of topology, chiral symmetry and confinement at high temperature has been investigated in many lattice studies. This review is devoted to the much less explored subject of topology in dense matter. After a short overview of the status at zero density, which will serve as a baseline for the discussion, we will present lattice results for baryon rich matter, which, due to technical difficulties, has been mostly studied in two-color QCD, and for matter with isospin and chiral imbalances. In some cases, a coherent pattern emerges, and in particular the topological susceptibility seems suppressed at high temperature for baryon and isospin rich matter. However, at low temperatures the topological aspects of dense matter remain not completely clear and call for further studies.

Keywords: QCD; topology; lattice field theory; dense matter; phase transitions

Citation: Lombardo, M.P. Topological Aspects of Dense Matter: Lattice Studies. *Universe* **2021**, *7*, 336. https://doi.org/10.3390/universe7090336

Academic Editor: Dmitri Antonov

Received: 31 July 2021
Accepted: 8 September 2021
Published: 9 September 2021

1. Introduction

In broad outline, the general framework of this review is Quantum Chromodynamics (QCD) and its several phases and critical phenomena depending on temperature, baryonic, isospin and chiral densities. At high temperatures the matter is in a plasma phase—the Quark-Gluon Plasma. At lower temperatures and increasing baryonic density, one encounters nuclear matter first, then a transition to a dense deconfined phase of quarks and gluons. This phase of matter is realised in the interior of neutron stars, extremely compact stellar objects produced in the supernova explosions. In this extreme environment several exotic phases can be realised. The recent observation of gravitational wave signals originating from the merging of two neutron stars has triggered further interest in the theoretical investigation in this direction, see e.g., Ref. [1].

Current and planned experiments have the capability of exploring the phase diagram of strong interactions. Ab-initio lattice studies [2,3] have produced results at non-zero baryon density, at rather large temperature in QCD, at non-zero isospin and chiral densities, and in entire phase diagram for two-color QCD, which is protected by the sign problem by the Pauli-Gürsey symmetry. The focus of most studies is on chiral and confining properties, and only a limited subset has addressed topology.

The interplay of chiral symmetry, confinement and topology may well depend on the details of the microscopic dynamics, which in turn is affected by matter density. In vacuum, chiral symmetry breaking occurs via a space-homogeneous condensate. At high temperature this is known to dissolve, while for low temperatures and high-density different pairing phenomena result in a rich, and still not entirely explored phase diagram [4–6]. In particular, Ref. [6] suggests a distinct different behaviour of the topological susceptibility at high temperatures and zero density, and high densities and low temperatures. A simplified view of the phase diagram from Ref. [5] can be seen in Figure 1. Non-homogeneous phases [7,8], predicted and only recently observed [9] in simple models at finite density, may well have different confining and topological properties.

A non-zero density—be it due to baryon, isospin or chiral imbalances—is then an important probe for the interplay of chiral symmetry, confinement and topology, and may shed some light on its general aspects.

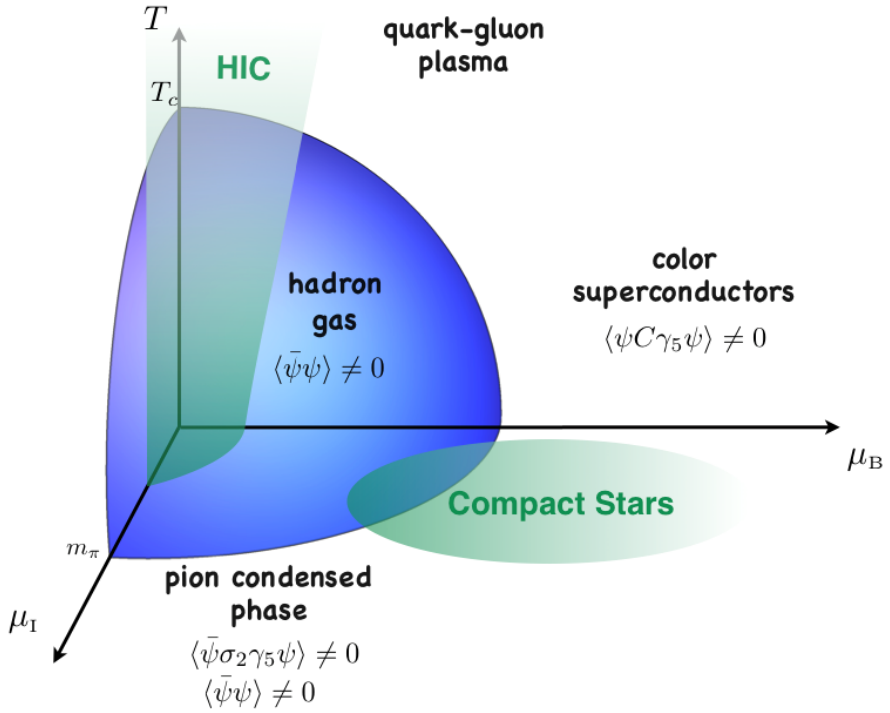

Figure 1. A schematic view of the phase diagram of QCD in the baryon, isospin chemical potential, and temperatures, from Ref. [5]. For two-color QCD the diagram would look similar, but the zero-temperature baryon and isospin critical chemical potential are the same, and the two dense phases are characterised by diquark and pion condensation.

2. Topology and Strong Interactions

The dynamics of gauge field is a fascinating aspect of strong interactions. Asymptotic freedom, and the self-interacting nature of the gluons, are reflected by the structure of the gauge sector of the theory. A configuration of gauge fields may have a topological content, measured by the topological charge density $q(x)$:

$$q(x) \equiv \frac{g^2}{32\pi^2} F^a_{\mu\nu} \tilde{F}^{\mu\nu}_a \tag{1}$$

Indeed (see e.g., Ref. [10]) $Q \equiv \int q(x) d^4x$ equals the Chern–Pontryagin index or winding number of gauge fields. It can only assume integer values, thus identifying the topological class to which the gauge configuration belongs.

The QCD Lagrangian may be coupled to the topological charge density

$$\mathcal{L} = \mathcal{L}_{QCD} + \theta \frac{g^2}{32\pi^2} F^a_{\mu\nu} \tilde{F}^{\mu\nu}_a, \tag{2}$$

Experiments on the electric dipole moment of the neutron d_n place limits on the value of θ parameter. The limits follow from the relation between d_n and θ. QCD sum rules give $d_n = 2.4 \times 10^{-16}\theta$ e cm [11] and chiral perturbation theory gives $d_n = 3.3 \times 10^{-16}\theta$ e cm [12]. The most recent experimental measure [13] of the neutron electric dipole moment is $d_n = (0.0 \pm 1.1\ (\text{stat}) \pm 0.2\ (\text{sys})) \times 10^{-26}$ e cm, which may be interpreted as an upper limit $|d_n| < 1.8 \times 10^{-26}$ e cm at a 90% C.L. Combining the experimental limit with the relations mentioned above, one arrives at the bound $\theta < 0.5 \times 10^{-10}$. This anomalously small value of θ leads to the hypothesis of an axion field which would force θ to vanish dynamically [14,15]. tealIn parallel, and not further discussed in this review, the possibility of a very small, but non-zero nEDM remains open. Such result would indicate physics

beyond the standard model [16] and it is a subject of an active theoretical investigation, see e.g., Ref. [17].

2.1. Topology, from Low to High Temperatures

The close and challenging interplay of topology, chiral and axial symmetry and gauge field dynamics—which we will briefly review below—has motivated investigations at high temperature, well before considering high density. In short summary, the topological susceptibility drops at the high temperature chiral phase transition, although it is still under debate whether a partial axial restoration coincides or not with chiral restoration, see e.g., Ref. [18] for a recent review, including a full set of references.

The behaviour of topology has been extensively studied at high temperature on the lattice [18–22]: it decreases in the plasma and at very high temperatures follows the predictions of the dilute instanton gas, DIGA (which we will briefly introduce in the next subsection), in which only configurations with zero, or unit, topological charges are possible. The results are briefly summarised in Figure 2, from Ref. [18].

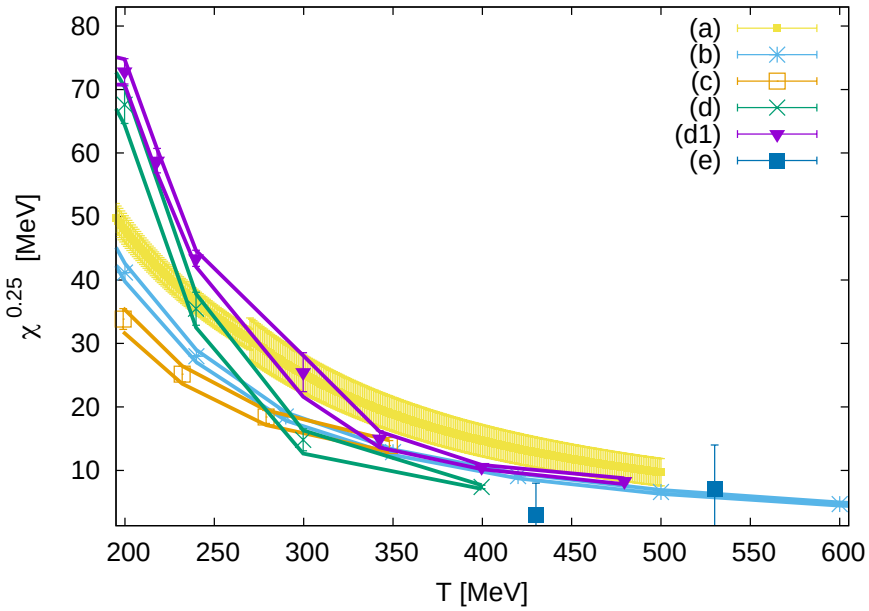

Figure 2. The fourth root of topological susceptibility versus the temperature in full QCD. (a) shows the gluonic results from Ref. [21]. (b) shows the tabulated results from Ref. [23]. (c) Ref. [24]; these results are rescaled from a higher pion mass (d) and (d1) show the results from Ref. [22] obtained by rescaling from the two lightest masses $m_\pi = 220, 260$ MeV. (e) the results from Ref. [20], where a careful continuum extrapolation with a conservative error estimate was performed. From Ref. [18].

2.2. Symmetries of QCD, and Topology

At a classical level, and in the massless limit, $\mathcal{L}_{QCD}$ has a global $U(N) \times U(N) \equiv SU(N) \times SU(N) \times U(1)_B \times U(1)_A$ symmetry, where N is the number of light flavours. The most natural scenario compatible with the pions and K mesons spectrum is the spontaneous breaking of the $SU(3) \times SU(3)$ symmetry of $\mathcal{L}_{QCD}$ in the three-flavour massless limit, while the other flavours are massive and do not participate in the chiral dynamics. In this scenario, Chiral Perturbation Theory predicts the masses of the mesons and baryons made by the physical up, down and strange quarks. The condensate formed in this breaking would also break the $U(1)_A$ symmetry: hence, the η' should follow the same fate as the other mesons, while it is distinctly heavier.

The way out is breaking explicitly the $U(1)_A$ symmetry [25]: since the topological charge appears in the divergence of the $U(1)_A$ current J_5^μ

$$\partial_\mu J_5^\mu = 2N_f Q + 2\sum_{i=1}^{N_f} m_i \bar{\psi}_i \gamma_5 \psi_i \tag{3}$$

the breaking of the axial symmetry may be achieved by a non-trivial topology which leads to the non-conservation of the current. In this way the large mass of the η' affords a direct evidence of the non-trivial topology of the vacuum, responsible for the explicit $U(1)_A$ breaking [26–28]. The η' carries thus interesting information on the anomalous component and on topology: as anticipated in Ref. [29] the η' should be on the same footing as the other mesons in the plasma, once the anomalous component disappears. Indeed, this was verified on the lattice in [30], see Figure 3.

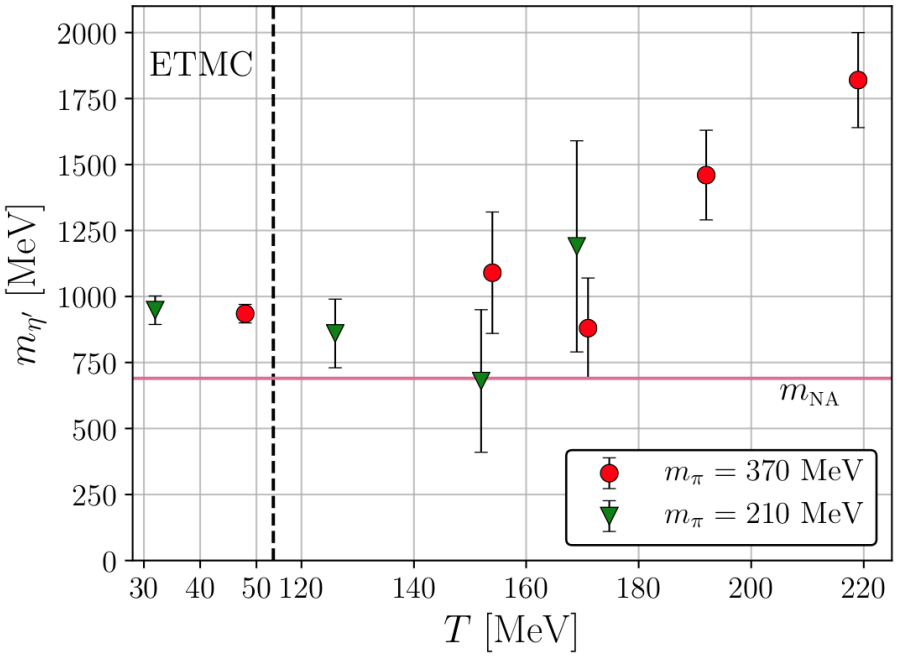

Figure 3. The mass of the η' as a function of the temperature in QCD: the η' mass approaches the mass of a (unphysical) $\bar{s}s$ meson at the transition, signaling the suppression of the anomalous component due to topological fluctuations. From Ref. [30].

Additionally, the spectrum results concurs in indicating that the topological susceptibility is greatly reduced in the plasma.

One interesting case, much studied numerically, is two-color QCD, which enjoys an enlarged chiral symmetry [31]: quarks and antiquarks belong to equivalent representation of the color group. As a consequence of that, the ordinary chiral symmetry of QCD $SU(N) \times SU(N)$ is enlarged to $SU(2N)$. Thanks to this symmetry the theory does not have a sign problem at non-zero baryon density: intuitively, baryon and isospin density are the same for the two-color world.

A further symmetry is the isospin symmetry: a global transformation, an $SU(2)$ rotation in flavour space (QCD interactions are flavour-blind). It acts on up and down quarks and $\mathcal{L}_{QCD}$ is invariant for identical or vanishing masses. In reality this symmetry is explicitly broken by the (small) mass difference between up and down quarks. Isospin breaking has consequences also on topology, since chiral perturbation theory [32] predicts, at leading order (LO),

$$\chi_{LO} = \frac{z}{1+z^2} m_\pi^2 f_\pi^2 \tag{4}$$

with $z = m_u/m_d$. We would not pursue these aspects—we will always consider $m_u = m_d$. We will instead consider the effect on topology of an isospin density [33], artificially induced by an appropriate chemical potential- more precisely, by its third component, I_3. The motivation for this is to understand the regime of finite density of a conserved charge (the isospin), aiming at the observation of the transition from hadronic to quark degrees of freedom at zero/low temperatures.

In nuclear matter and in astrophysics isospin imbalance is very important, however in real world the baryonic density is much larger than the isospin one, $\mu_I \ll \mu_B$. In Ref. [33] as well as in lattice studies [34–40], the authors consider an idealization with $\mu_I \neq 0, \mu_B = 0$. Such a system is unstable under weak interactions which do not conserve isospin. Nonetheless, in this purely QCD world this system can still give us relevant information, also considering that it is free from the sign problem [31], and we will discuss lattice results below.

This brief discussion on symmetries leads us to consider three different chemical potentials: two of which associates with conserved charges, μ_B and μ_I, the third associated with a the non-conserved axial current, $\mu_5 \equiv (\mu_R - - - \mu_L)/2$, which couples to the current $\bar{\psi}_i \gamma_5 \psi_i$ see Equation (3).

2.3. Conserved Charges μ_B and μ_I

Let us consider again the phase diagram in the μ_B, μ_I, T space, from Ref. [5], see Figure 1: at high temperature-chiral symmetry is restored. In the limit of zero temperatures isospin and baryochemical potential induce the transition to a dense phase, characterised by different pairing phenomena, see e.g., Refs. [4,5]. A standard scenario predicts the transition when the chemical potential equals the mass of the lowest state carrying the corresponding charge: $\mu_B^c \simeq m_N$, and $\mu_I^c \simeq m_\pi$, with m_N and m_π being the nucleon and pion mass, respectively. The two dense phases are characterised by different pairing phenomena in real QCD, and are probably separated by a low temperature phase transition at in the μ_B, μ_I plane, studied in chiral perturbation theory [41].

In two-color QCD, due to the already mentioned fact that the baryons of the theory are diquarks, the phase diagram in Figure 1 would look the same in the two directions, with the same thresholds along baryon and isospin chemical potential. The two condensed phases, which are significantly different in QCD, are now the same and have both (colorless) condensates: diquark and pion condensates in the μ_B and μ_I directions.

2.4. Instantons and Zero Modes

One possible way to discuss the different properties of the phases of strong interactions at zero and non-zero density vis-a-vis topology is to consider the behaviour of instantons [42]. Instantons are classical solutions to the Euclidean equations of motion: localized regions of space-time (typical sizes are 1/3 fm) , with very strong gluonic fields, and characterised by a topological quantum number. It turns out that there are important differences in the instanton behaviour at zero and non-zero densities and temperatures [6,43,44]. At low temperatures one expects a random instanton ensemble, accounting for chiral breaking. At high temperatures one expects instanton-anti-instanton pairs, eventually behaving at high temperatures like a dilute gas, described by the Dilute Instanton Gas Approximation, DIGA, in which only configurations with zero, or unit, topological charges are possible, while at finite density one may expect instanton chains [43]. The reason for this [43] is that either at finite temperature and finite density the quark propagation in time direction is favored over space-like propagation, the latter being suppressed by $e^{-\pi T r}$ and $e^{i\mu r}$, respectively. In general, the fermion determinant generates strong correlations among instantons. Because of this, the random instanton ensemble, responsible for chiral breaking, dissolves into clusters oriented in the time direction: the already mentioned instanton-anti-instanton pairs at high temperature (eventually turning into the dilute instanton gas) and instanton chains at high density.

The details may be found in Ref. [44], where the authors discuss the role of instantons in the three major phases of strong interactions: the hadronic phase, the color superconductor phase, and the quark-gluon plasma phase. In brief, the reasoning starts from Equation (3) which shows a remarkable connection between gauge fields and fermions. This is made more transparent by the Atiyah–Singer index theorem [45,46]:

$$\frac{1}{32\pi^2}\,\varepsilon_{\mu\nu\rho\sigma}\int \mathrm{Tr}[F^{\mu\nu}(x)F^{\rho\sigma}(x)]\,d^4x = n_+ - n_-\,. \tag{5}$$

We see that the topological charge 'counts' the number of zero modes of the massless Dirac operator with positive and negative chirality $n_\pm$. The Atiyah–Singer theorem works also at finite density, however, the nature of the zero modes are now different, since there are extra states appearing at the Fermi surface. In QCD this interaction leads to the formation of diquark (colored) Cooper pairs, to BCS instability and to color superconductivity—these are the phases depicted in Figure 1. In two-color QCD, diquark pairs are stable as they are color neutral and a diquark condensate is formed. The different phases of strong interactions can then be characterised by instanton dynamics, and an important point is that pair dynamics should always predominate as temperature increases, at any chemical potential. One would then expect some significant changes in topology at fixed chemical potential when increasing temperature, as well as changes when fixing the temperature and increasing the chemical potentials.

2.5. *Detecting Topology—The Chiral Magnetic Effect and* μ_5

From a phenomenological point of view, the Atiyah–Singer theorem opens the way to the possibility of a direct observation of topology in experiments, see e.g., Refs. [47–49]. In fact, the gluons do not carry conserved charges which could be directly measured. But we can still 'see' topological fluctuations in the quark sector. These observations are at the root of the discovery of the so-called Chiral Magnetic Effect (CME) [49]: electric charge separation in the presence of an external magnetic field that is induced by the chirality imbalance. This striking effect could be observed in heavy ion collisions and in condensed matter experiments and its prediction has spawned a significant experimental activity. Many reviews are available, see e.g., [48] and we will not discuss further the CME here, as our focus is equilibrium studies of topology and their signatures in the phase diagram. However, it is important to underscore that it is indeed the CME that has called the attention of the lattice community on the chiral chemical potential, and has motivated the numerical analysis at equilibrium which we will discuss later. teal It is important to notice that the chiral chemical potential μ_5 couples to the chiral charge density operator $\psi^\dagger\gamma_5\psi$ which is not conserved because of the chiral anomaly. So it is not on the same footing as the baryon chemical potential or the isospin chemical potential. μ_5 cannot be generated in thermodynamic equilibrium, topological fluctuations will wash it out: μ_5 is just an external coupling able to generate a chiral imbalance [50–54], and it may require renormalization in the ultraviolet [50].

3. Lattice Results—Topology and Dense Matter

In the previous Section we have argued that one may expect some significant differences in topology in the different phases, and have shown a summary of results at zero density. Here we will review the current lattice results for topology in dense matter, with different temperatures.

A very brief technical note before proceeding: let us remind ourselves that the different densities we have discussed are realised by adding the appropriate zeroth component of the current to the Lagrangian, while on Euclidean lattices the temperature is the reciprocal of the time extent of the lattice, $T = 1/N_t a$, a being the lattice spacing and N_t the number of sites in the temporal direction. The results on topology are so far limited to the topological susceptibility, the fluctuations of the topological charge. Details on the rich and highly technical subject of lattice topology may be found in Ref. [55].

3.1. Baryon Density

These studies were mostly carried out for two-color QCD, since this is free from the sign problem. As discussed above, the dynamics may be significantly different from that of QCD, especially concerning the nature of the pairing at high density. However, the hope is that the main features of instanton dynamics which are at the heart of this discussion remain valid—although of course this is subject to verification.

Studies of two-color matter have been performed by several groups [34,56–64]. teal In cold matter, these studies have confirmed that baryonic matter forms at an onset $\mu_o = m_\pi/2$, whereupon diquarks start populating the vacuum. If the dynamics favor pairing, they could condense: diquark condensation at low temperatures, above μ_o is consistently observed in lattice studies. However, the dependence of the diquark condensate on the chemical potential is still unsettled, leading to different hypotheses on the nature of the phase about μ_o: some studies find consistence with chiral perturbation theory indicating a BEC phase [64], followed from a transition to free behaviour, interpreted as a crossover to BCS. Others find compatibility with a free quark behaviour [65] immediately above μ_o, at largish masses, and non-conclusive results for lower masses [65]. According to the same study, early signals for deconfinement for chemical potentials $\mu \simeq 1.1 m_\pi$ [61] should be interpreted with care. In brief, the issue of the nature of the dense phase above μ_o is subtle, and under investigation. The very existence of an onset at μ_o and low temperatures is instead uncontroversial, and we will concern ourselves with the behaviour of topology past this onset, in comparison with the observations at high temperatures.

One first study of topology was carried out in two-color QCD with eight flavours of staggered fermions [58]—this choice may be surprising as the theory in the continuum limit is known to be within the conformal window of QCD, see e.g., Refs. [66–68]. However, the coupling was strong enough to break chiral symmetry at zero temperature. In this condition one may study the phase diagram—similarly, for instance, to what one would do in lattice strong coupling electrodynamics. One important caveat, of course, is that topology is poorly defined at strong coupling: the very nature of the topology require the continuum limit [55]—on a discrete system the barriers among different topological sectors are finite, as the system may be easily deformed. On the lattice, this produces the so-called dislocations, which artificially increase topological fluctuations. To mitigate, at least partially, this effect in Ref. [58] the analysis is restricted to finite temperature, which is realised with finer lattices. In addition to that, the lattice configurations were subjected to smoothing—a local coarse graining—designed to suppress artifacts. The results of [58] indicate that gluon dynamics, chiral symmetry and topology are interrelated in the region of temperatures $0.3 < T/T_c < 0.4$. The behaviour is exemplified in Figure 4: to appreciate the correlation among different observables the diagrams show the derivatives with respect to the chemical potential of the Polyakov loop, the chiral condensate and the topological susceptibility. The coincidence of the peaks, signaling the onset of the superfluid phase, is quite clear.

Obviously, these earlier investigations called for more studies, including lower temperatures. Of particular interest would be the study of topology in the superfluid phase, characterised by a diquark condensate, as discussed at the beginning of this Section.

A study dedicated to topology in the cold phase, i.e., accessing the superfluid region of two-color QCD, found interesting differences between two and four flavours [61], see Figure 5. The topological susceptibility was measured on two different gauge field ensembles. The first used a $12^3 \times 24$ lattice and $N = 2$ flavours of Wilson fermions. The second ensemble used the same system size, and $N = 4$. The two ensembles have similar pion masses in lattice units, $m_\pi a = 0.68$, and may be considered fairly 'cold': the onset for the superfluid phase should then be $\mu_o a \simeq 0.34$. A summary of the results is offered by Figure 5: interestingly, apparently the topology in the two-flavour theory is insensitive to the chemical potential, while the results in the four-flavour model may even suggest an increase of the topological susceptibility. The authors issue a caveat though: also, in this case one may fear important discretization effects. Barring these, the observation is

that other thermodynamic studies revealed that the two-flavour model is weakly coupled above the onset [60], while in contrast, the four-flavour model appears to be strongly coupled [62]. So, there is the possibility that the raise of the topological susceptibility in the four-flavour model above the onset does indeed reflect the strongly coupled nature of the theory.

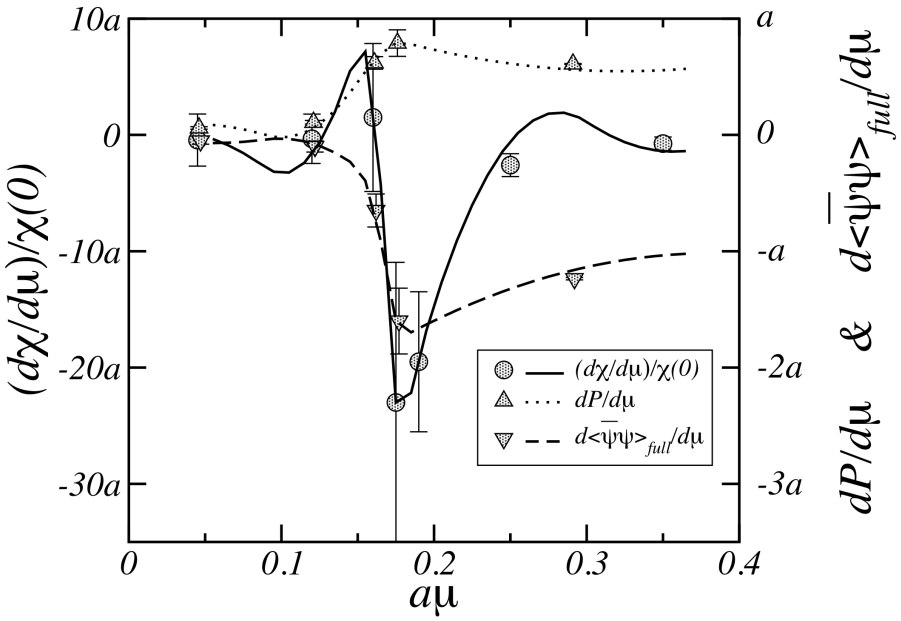

Figure 4. The correlation among topology, confinement and chiral symmetry as seen from the μ_B derivatives of the topological susceptibility, the Polyakov loop and the chiral condensate in two-color QCD, on a hot lattice. From Ref. [58].

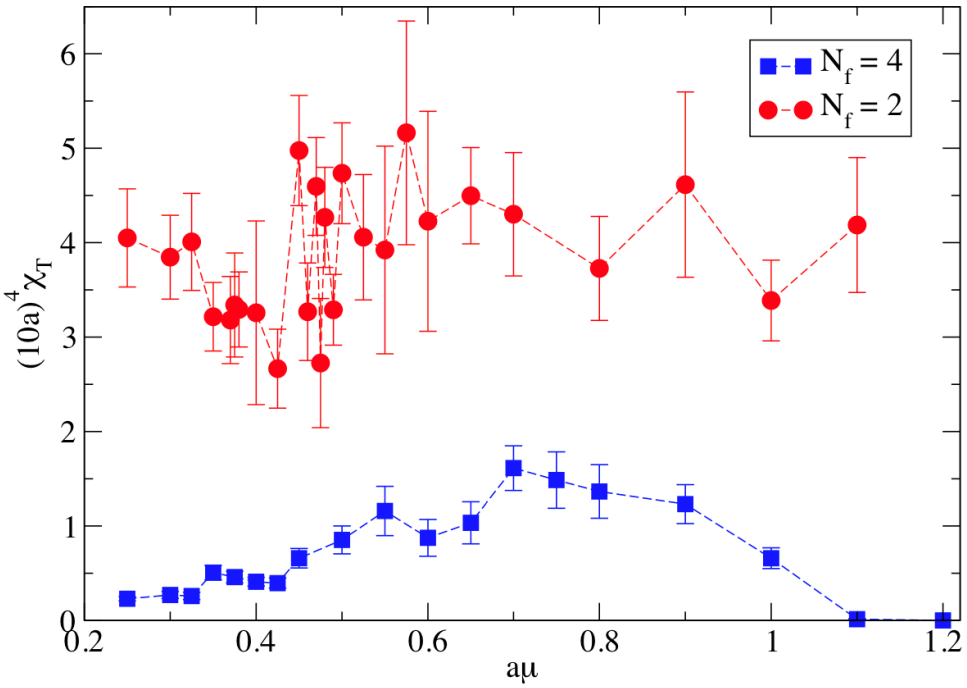

Figure 5. Topological susceptibility versus chemical potential in two-color QCD for two and four flavours, from Ref. [61], in a cold lattice; the expected μ_o in lattice units is $\mu_o a \simeq 0.34$.

A recent paper [64] analysed the temperature dependence of the results at high chemical potential using the same setup at low and high temperature, but for the number of time slices, which controls the temperature itself. At a temperature of about $0.45T_c$, where T_c is the chiral transition temperature at zero chemical potential, the topological susceptibility is found to be almost constant for all the values of chemical potential, from the hadronic to superfluid phase. In contrast, for a temperature of about $0.89T_c$ the topological susceptibility becomes small as the hadronic phase changes into the quark-gluon plasma phase. The results, shown in Figure 6, indicate a significant temperature effect, which changes the behaviour of the topological susceptibility from constant with μ_B (in the cold phase) to decreasing with μ in the hot phase, the latter observation in agreement with Ref. [57].

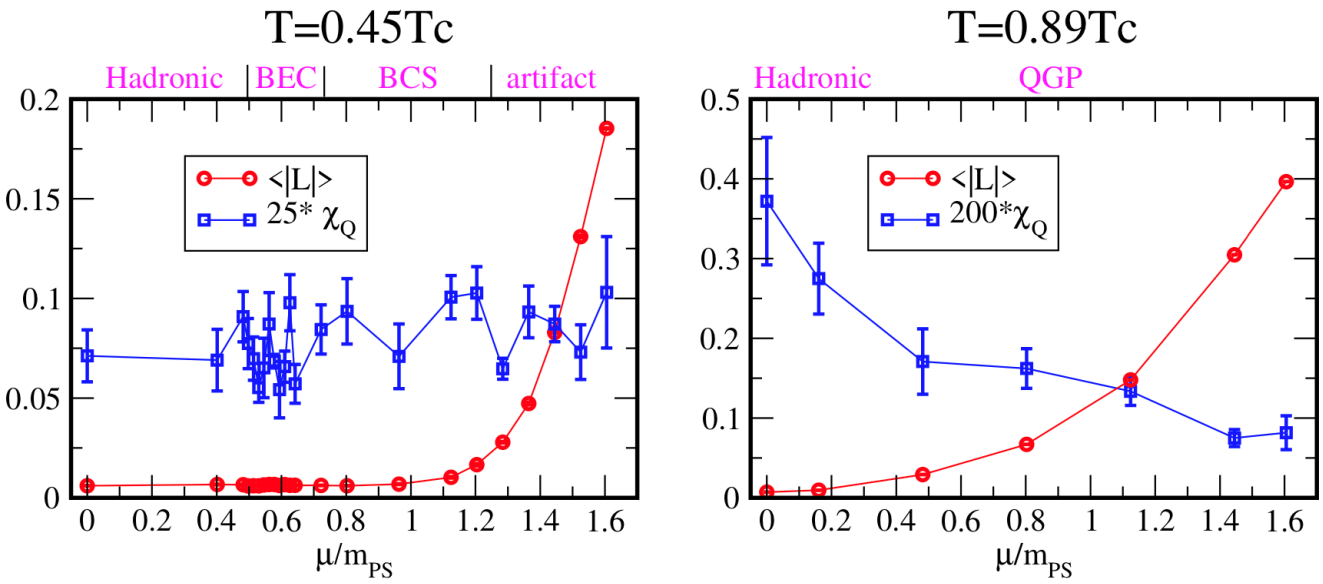

Figure 6. Polyakov loop and topological susceptibility in two-color QCD, in a cold (**left**) and in hot lattice, from Ref. [64]. We would like to highlight here the lack of sensitivity of the topological susceptibility on the threshold for the Polyakov loop at μ_o at $T = 0.45T_c$ (**left**), to be contrasted with the (anti) correlated behaviour of the same observables in the Quark-Gluon Plasma (**right**). Please note that the identification of the diquark dense phase with a BEC phase followed by a BCS one is still under debate [65].

The results of [34] are obtained on a 32^4 lattice, which is described as a cold one. In simulations for $N = 2$ a clear correlation between chiral condensate and topological susceptibility emerged Figure 7. Accepting that these are simulations on cold lattices, there is an apparent contradiction with the scenario of [62,64], see Figure 6, left, as well Figure 5, left. However, the physical temperature is, according to the estimates of the paper $T = 140$ MeV [34], so it could well be that one is effectively observing a transition to a Quark-Gluon Plasma, albeit in a finite volume. Indeed the diquark condensate remains smaller than the condensate, indicating a different behaviour from the cold transition. This may offer a solution to this apparent puzzle. A clearer conclusion may be reached by performing simulations for chemical potentials in the dense phase, and varying temperatures: one may observe a transition from a phase with large topological susceptibility to a phase with suppressed susceptibility. Lacking those simulations, for the time being the results remain to some extent puzzling.

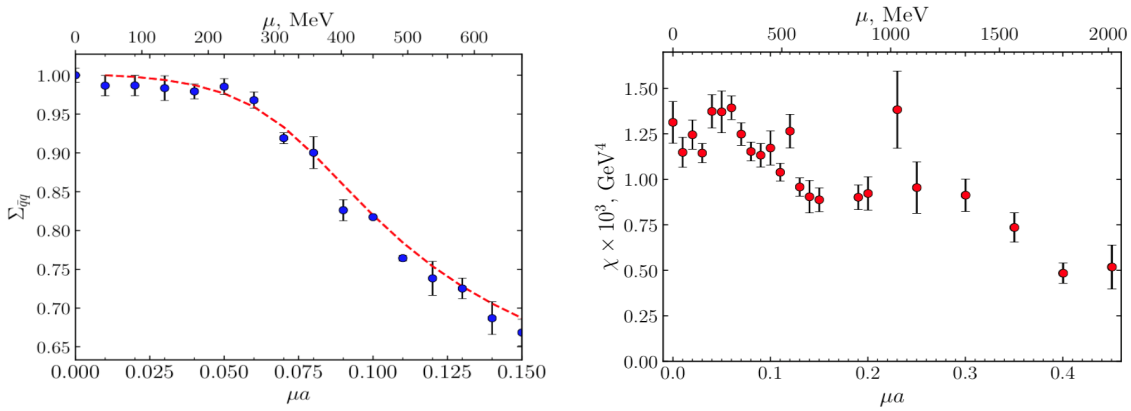

Figure 7. Chiral condensate and topological susceptibility as a function of baryochemical potential in two-color QCD, from Ref. [34].

3.2. Isospin Density

The phase diagram at finite density of isospin, introduced in Section 2 and shown in Figure 8, has been studied on the lattice by various authors [36,38,69,70]. An interesting feature is that the critical line $T = T(\mu_I)$ has a very small slope—it is almost horizontal. So simulations performed at fixed temperature varying μ_I are very likely crossing the pion condensation line unless the temperature is really close to T_c.

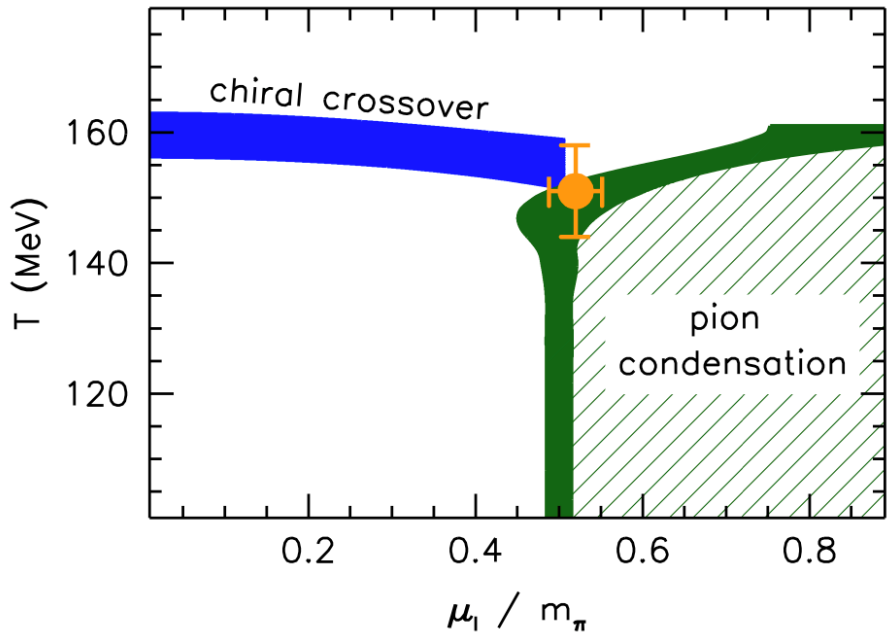

Figure 8. Lattice results for the phase diagram of QCD in the temperature-chemical potential for isospin plane, from Ref. [36].

Topology was studied in Ref. [71]: the authors perform simulations in full QCD with staggered fermions on $24^3 \times 6$ lattices, with a similar setup as the one used in Ref. [72] to study a 8^4 lattice. In Ref. [72] the transition to the condensed phase was clearly observed, with $\mu_I^c \simeq m_\pi/2$ On the $24^3 \times 6$ lattice the pion mass was set at its physical value, corresponding to $m_\pi a = 0.2$, leading to an expected critical isospin chemical potential $\mu_I^c a = 0.1$. Topology was then studied by analysing the zero and non-zero modes of the overlap Dirac operator, which has an exact chiral symmetry, and it is thus particularly suited for this analysis. The eigenvalue distributions were obtained for $\mu_I = 0.5, 1.5\mu_{I_c}$

i.e., below and above the isospin phase transition, and they are remarkably similar, see Figure 9.

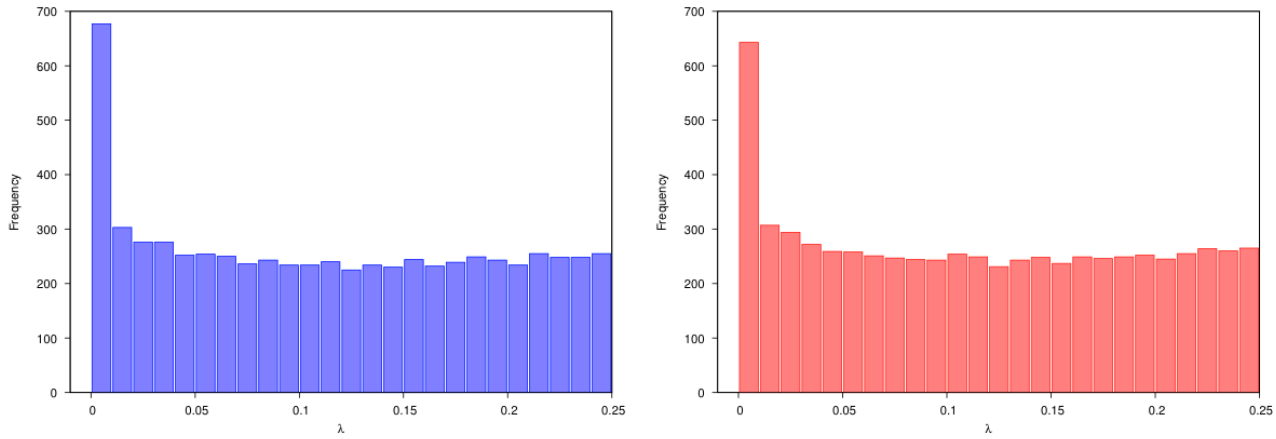

Figure 9. Eigenvalue spectrum of the Overlap Dirac operator for QCD with a physical pion mass, on $24^3 \times 6$ lattice for $\mu_I = 0.5, 1.5\mu_{I_c}$, left and right diagram. From Ref. [71].

As with what was observed at finite baryon density, and low temperatures, in two-color QCD, apparently topology in cold systems does not change in dense matter. This would be consistent with the predictions of Ref. [6].

3.3. Chiral Density

Early lattice studies of chiral density were performed having in mind a toy model for the chiral magnetic effect in heavy ion collisions [52]. One first systematic study of the phase diagram at equilibrium appeared in Ref. [73]. Even if QCD with a chiral density does not have a sign problem, these first studies were performed for two-color QCD, for the sake of simplicity, economy of computational resources , and possible comparison with results in two-color QCD with a magnetic field. The resulting phase diagram—which confirms the prediction of model studies—is reproduced in Figure 10. The larger extent of the hadronic phase—T_c increases with μ_5—reflects the so-called chiral catalisys [53]—the enhancement of the chiral condensate due to chiral imbalance, which pushes the critical temperatures towards higher values when increasing μ_5. Details and a rich list of references may be found in a recent review [54].

Lattice studies of topology and confinement with a chiral imbalance have been performed in QCD in Ref. [51], using the tree level improved Symanzik gauge action and staggered fermions with two flavours of dynamical quarks. Four different pion masses were explored: $m_\pi = (563, 762, 910)$ MeV. It was found that the model follows the chiral perturbation theory prediction [74] $\rho_5 = \Lambda_{QCD}\mu_5$: the chiral density depends linearly on the chiral chemical potential, there are no thresholds. The study reveals that the topological susceptibility increases with the chiral chemical potential, much in the same way as the chiral condensate did in the two-color study. Moreover, also the string tension increases, in a rather correlated way. This was interpreted [51] as a signal that the chiral chemical potential leads to larger fluctuations of the chiral density and, due to the anomaly, to larger topological fluctuations in QCD: the chiral chemical potential enhances topological fluctuations which in turn are related to the strength of confinement as seen from the string tension, see Figure 11.

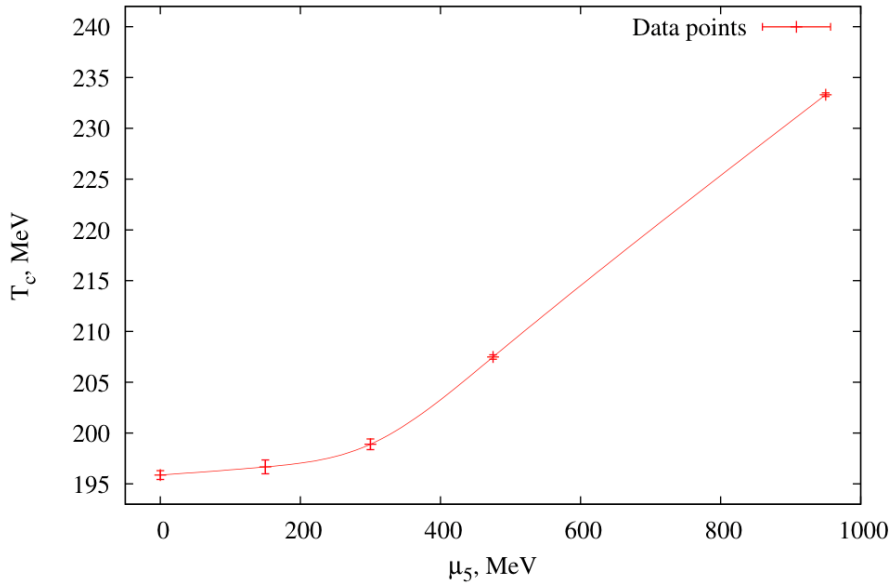

Figure 10. The phase diagram of QCD (two-color) in the temperature-chiral chemical potential plane; note the enlargement of the hadronic phase due to the enhancement of chiral breaking. From Ref. [73].

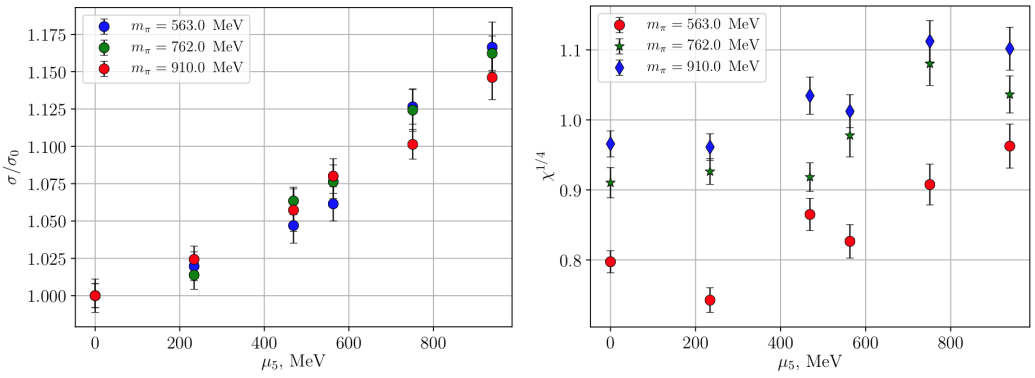

Figure 11. String tension (**left**) and topological susceptibility (**right**) in QCD as a function of the chiral chemical potential, and different pion masses. From Ref. [51].

4. Summarising

Topology and dense matter are studied independently, and intensively on the lattice. However, studies of the topological aspects in dense matter are still relatively scarce. We have reviewed the available information for a baryon rich matter, mostly coming from two-color QCD, for isospin dense matter, and for a chiral imbalance, hoping to highlight some clear trend, and to contribute to identify the open issues.

Actually, none of the systems considered here is completely realistic: finite baryon density may well be realised in experiments; however, on the lattice one must use (unphysical) theories free from the sign problem to access to cold, dense phase. Dense, baryon-less isospin matter would be unstable under weak interactions. Additionally, chiral imbalance does not exist at equilibrium even in strong interactions. Yet, these studies may add to our understanding of the phases of strong interactions, and , in some cases, pose some new challenge. Indeed, one of the main points to be addressed—the interrelation among topology, confinement, chiral symmetry—remains to large extent unsolved. These ambiguities are partly due to lattice artifacts—they are highlighted in all the works we have reviewed, partly to the different setup of the simulations.The ambiguities may be particularly severe in systems with a chiral chemical potential, which are to some extent artificial, and where a continuum limit is not well defined. Very few studies are available in which dense matter has been explored as a function of temperature within the same model.

Nonetheless, at least at high temperature, some coherent pattern emerges: a tentative conclusion is that above the critical temperature for superfluidity/superconductivity, the topological susceptibility as a function of chemical potential, either isospin and baryonic, is well correlated with the chiral condensate and the signals for confinement. The same remains true for the chiral chemical potential: in that case, there is a striking effect called chiral enhancement: the chiral condensate grows with chemical potential—and the same is true for topological susceptibility and string tension.

At low temperatures, however, the results for the topological susceptibility are not entirely settled: in some cases, a similar behaviour as high temperature has been reported; in other cases a sensitivity to the number of flavours has been observed; other studies conclude for the insensitivity of the topological susceptibility to the matter density. The latter observation would indeed be consistent with the analysis of Ref. [6]. The results in cold systems often call for further investigations and better control of the lattice artifacts, and this may be particularly true for studies with a chiral chemical potential. This said, a feature which seems to be well established is the insensitivity of topological susceptibility to dense matter. However, if instantons' chains were indeed realised in cold and dense matter, there should be some signatures in topological observables. Should one think that the behaviour of topological susceptibility invalidates this picture, or, rather, that topological susceptibility is simply not able to capture it?

Funding: This work is partially supported by STRONG-2020, a European Union's Horizon 2020 research and innovation programme under grant agreement No. 824093.

Conflicts of Interest: The author declares no conflict of interest.

References

1. Dexheimer, V.; Constantinou, C.; Most, E.R.; Jens Papenfort, L.; Hanauske, M.; Schramm, S.; Stoecker, H.; Rezzolla, L. Neutron-Star-Merger Equation of State. *Universe* **2019**, *5*, 129. [CrossRef]
2. Ratti, C. Lattice QCD and heavy ion collisions: A review of recent progress. *Rept. Prog. Phys.* **2018**, *81*, 084301. [CrossRef] [PubMed]
3. Guenther, J.N. Overview of the QCD phase diagram: Recent progress from the lattice. *Eur. Phys. J. A* **2021**, *57*, 136. [CrossRef]
4. Rajagopal, K.; Wilczek, F. The Condensed matter physics of QCD. *Front. Part. Phys. Handb. QCD* **2000**, *11*, 2061–2151 .
5. Mannarelli, M. Meson condensation. *Particles* **2019**, *2*, 411–443. [CrossRef]
6. Pisarski, R.D.; Rennecke, F. Multi-instanton contributions to anomalous quark interactions. *Phys. Rev. D* **2020**, *101*, 114019. [CrossRef]
7. McLerran, L.; Redlich, K.; Sasaki, C. Quarkyonic Matter and Chiral Symmetry Breaking. *Nucl. Phys. A* **2009**, *824*, 86–100. [CrossRef]
8. Buballa, M.; Carignano, S. Inhomogeneous chiral condensates. *Prog. Part. Nucl. Phys.* **2015**, *81*, 39–96. [CrossRef]
9. Buballa, M.; Kurth, L.; Wagner, M.; Winstel, M. Regulator dependence of inhomogeneous phases in the (2+1)-dimensional Gross-Neveu model. *Phys. Rev. D* **2021**, *103*, 034503. [CrossRef]
10. Jackiw, R.W. Axial anomaly. *Scholarpedia* **2008**, *3*, 7302. [CrossRef]
11. Pospelov, M.; Ritz, A. Theta vacua, QCD sum rules, and the neutron electric dipole moment. *Nucl. Phys. B* **2000**, *573*, 177–200. [CrossRef]
12. Pich, A.; de Rafael, E. Strong CP violation in an effective chiral Lagrangian approach. *Nucl. Phys. B* **1991**, *367*, 313–333. [CrossRef]
13. Abel, C.; Afach, S.; Ayres, N.J.; Baker, C.A.; Ban, G.; Bison, G.; Bodek, K.; Bondar, V.; Burghoff, M.; Chanel, E.; et al. Measurement of the permanent electric dipole moment of the neutron. *Phys. Rev. Lett.* **2020**, *124*, 081803. [CrossRef] [PubMed]
14. Peccei, R.D.; Quinn, H.R. CP Conservation in the Presence of Instantons. *Phys. Rev. Lett.* **1977**, *38*, 1440–1443. [CrossRef]
15. Peccei, R.D.; Quinn, H.R. Constraints Imposed by CP Conservation in the Presence of Instantons. *Phys. Rev. D* **1977**, *16*, 1791–1797. [CrossRef]
16. Pospelov, M.; Ritz, A. Electric dipole moments as probes of new physics. *Ann. Phys.* **2005**, *318*, 119–169. [CrossRef]
17. Alexandrou, C.; Athenodorou, A.; Hadjiyiannakou, K.; Todaro, A. Neutron electric dipole moment using lattice QCD simulations at the physical point. *Phys. Rev. D* **2021**, *103*, 054501. [CrossRef]
18. Lombardo, M.P.; Trunin, A. Topology and axions in QCD. *Int. J. Mod. Phys. A* **2020**, *35*, 2030010. [CrossRef]
19. Borsanyi, S.; Dierigl, M.; Fodor, Z.; Katz, S.D.; Mages, S.W.; Nogradi, D.; Redondo, J.; Ringwald, A.; Szabo, K.K. Axion cosmology, lattice qcd and the dilute instanton gas. *Phys. Lett.* **2016**, *752*, 175–181. [CrossRef]
20. Bonati, C.; D'Elia, M.; Martinelli, G.; Negro, F.; Sanfilippo, F.; Todaro, A. Topology in full QCD at high temperature: A multicanonical approach. *J. High Energy Phys.* **2018**, *11*, 170. [CrossRef]

21. Petreczky, P.; Schadler, H.; Sharma, S. The topological susceptibility in finite temperature QCD and axion cosmology. *Phys. Lett. B* **2016**, *762*, 498–505. [CrossRef]
22. Burger, F.; Ilgenfritz, E.-M.; Lombardo, M.P.; Trunin, A. Chiral observables and topology in hot QCD with two families of quarks. *Phys. Rev. D* **2018**, *98*, 094501. [CrossRef]
23. Borsányi, S.; Fodor, Z.; Guenther, J.; Kampert, K.H.; Katz, S.D.; Kawanai, T.; Kovacs, T.G.; Mages, S.W.; Pasztor, A.; Pittler, F.; et al. Calculation of the axion mass based on high-temperature lattice quantum chromodynamics. *Nature* **2016**, *539*, 69–71. [CrossRef]
24. Taniguchi, Y.; Kanaya, K.; Suzuki, H.; Umeda, T. Topological susceptibility in finite temperature (2+1)-flavor QCD using gradient flow. *Phys. Rev. D* **2017**, *95*, 054502. [CrossRef]
25. Weinberg, S. The U(1) Problem. *Phys. Rev. D* **1975**, *11*, 3583–3593. [CrossRef]
26. Vecchia, P.D.; Veneziano, G. Chiral Dynamics in the Large n Limit. *Nucl. Phys. B* **1980**, *171*, 253–272. [CrossRef]
27. Vecchia, P.D.; Giannotti, M.; Lattanzi, M.; Lindner, A. Round Table on Axions and Axion-like Particles. *PoS Confin.* **2019**, *2018*, 034.
28. Veneziano, G. U(1) Without Instantons. *Nucl. Phys. B* **1979**, *159*, 213–224. [CrossRef]
29. Kapusta, J.I.; Kharzeev, D.; McLerran, L.D. The Return of the prodigal Goldstone boson. *Phys. Rev. D* **1996**, *53*, 5028–5033. [CrossRef] [PubMed]
30. Kotov, A.Y.; Lombardo, M.P.; Trunin, A.M. Fate of the η' in the quark gluon plasma. *Phys. Lett. B* **2019**, *794*, 83–88. [CrossRef]
31. Alford, M.G.; Kapustin, A.; Wilczek, F. Imaginary chemical potential and finite fermion density on the lattice. *Phys. Rev. D* **1999**, *59*, 054502. [CrossRef]
32. Gorghetto, M.; Villadoro, G. Topological Susceptibility and QCD Axion Mass: QED and NNLO corrections. *J. High Energy Phys.* **2019**, *2019*, 033. [CrossRef]
33. Son, D.T.; Stephanov, M.A. QCD at finite isospin density. *Phys. Rev. Lett.* **2001**, *86*, 592–595. [CrossRef]
34. Astrakhantsev, N.; Braguta, V.V.; Ilgenfritz, E.M.; Kotov, A.Y.; Nikolaev, A.A. Lattice study of thermodynamic properties of dense QC_2D. *Phys. Rev. D* **2020**, *102*, 074507. [CrossRef]
35. Brandt, B.B.; Cuteri, F.; Endrődi, G.; Schmalzbauer, S. The Dirac spectrum and the BEC-BCS crossover in QCD at nonzero isospin asymmetry. *Particles* **2020**, *3*, 80–86. [CrossRef]
36. Brandt, B.B.; Endrodi, G.; Schmalzbauer, S. QCD phase diagram for nonzero isospin-asymmetry. *Phys. Rev. D* **2018**, *97*, 054514. [CrossRef]
37. Brandt, B.B.; Cuteri, F.; Endrodi, G.; Schmalzbauer, S. Exploring the QCD phase diagram via reweighting from isospin chemical potential. *PoS LATTICE* **2019**, *2019*, 189.
38. Braguta, V.V.; Kotov, A.Y.; Nikolaev, A.A. Lattice Simulation Study of the Properties of Cold Quark Matter with a Nonzero Isospin Density. *JETP Lett.* **2019**, *110*, 1–4. [CrossRef]
39. Detmold, W.; Orginos, K.; Shi, Z. Lattice QCD at non-zero isospin chemical potential. *Phys. Rev. D* **2012**, *86*, 054507. [CrossRef]
40. Cea, P.; Cosmai, L.; D'Elia, M.; Papa, A.; Francesco Sanfilippo The critical line of two-flavor QCD at finite isospin or baryon densities from imaginary chemical potentials. *Phys. Rev. D* **2012**, *85*, 094512. [CrossRef]
41. Toublan, D.; Kogut, J.B. Isospin chemical potential and the QCD phase diagram at nonzero temperature and baryon chemical potential. *Phys. Lett. B* **2003**, *564*, 212–216. [CrossRef]
42. Schäfer, T.; Shuryak, E.V. Instantons in qcd. *Rev. Mod. Phys.* **1998**, *70*, 323–425. [CrossRef]
43. Rapp, R.; Schäfer, T.; Shuryak, E.V.; Velkovsky, M. Diquark Bose condensates in high density matter and instantons. *Phys. Rev. Lett.* **1998**, *81*, 53–56. [CrossRef]
44. Rapp, R.; Schäfer, T.; Shuryak, E.V.; Velkovsky, M. High density QCD and instantons. *Ann. Phys.* **2000**, *280*, 35–99. [CrossRef]
45. Atiyah, M.F.; Singer, I.M. The Index of elliptic operators. 5. *Ann. Math.* **1971**, *93*, 139–149. [CrossRef]
46. Atiyah, M.F.; Singer, I.M. Dirac Operators Coupled to Vector Potentials. *Proc. Natl. Acad. Sci. USA* **1984**, *81*, 2597–2600. [CrossRef]
47. Bzdak, A.; Esumi, S.; Koch, V.; Liao, J.; Stephanov, M.; Xu, N. Mapping the Phases of Quantum Chromodynamics with Beam Energy Scan. *Phys. Rept.* **2020**, *853*, 1–87. [CrossRef]
48. Kharzeev, D.E.; Levin, E.M. Color Confinement and Screening in the θ Vacuum of QCD. *Phys. Rev. Lett.* **2015**, *114*, 242001. [CrossRef] [PubMed]
49. Kharzeev, D.E. The chiral magnetic effect and anomaly-induced transport. *Prog. Part. Nucl. Phys.* **2014**, *75*, 133–151. [CrossRef]
50. Ruggieri, M.; Chernodub, M.N.; Lu, Z. Topological susceptibility, divergent chiral density, and phase diagram of chirally imbalanced QCD medium at finite temperature. *Phys. Rev.* **2020**, *102*, 014031. [CrossRef]
51. Astrakhantsev, N.Y.; Braguta, V.V.; Kotov, A.Y.; Kuznedelev, D.D.; Nikolaev, A.A. Lattice study of QCD at finite chiral density: Topology and confinement. *Eur. Phys. J. A* **2021**, *57*, 15. [CrossRef]
52. Yamamoto, A. Chiral magnetic effect in lattice qcd with a chiral chemical potential. *Phys. Rev. Lett.* **2011**, *107*, 031601. [CrossRef] [PubMed]
53. Braguta, V.V.; Kotov, A.Y. Catalysis of dynamical chiral symmetry breaking by chiral chemical potential. *Phys. Rev.* **2016**, *93*, 105025. [CrossRef]
54. Yang, L.; Luo, X.; Segovia, J.; Zong, H. A Brief Review of Chiral Chemical Potential and Its Physical Effects. *Symmetry* **2020**, *12*, 2095. [CrossRef]
55. Müller-Preussker, M. Recent results on topology on the lattice (in memory of Pierre van Baal). *PoS LATTICE* **2015**, *2014*, 003.
56. Hands, S.; Kogut, J.B.; Lombardo, M.; Morrison, S.E. Symmetries and spectrum of SU(2) lattice gauge theory at finite chemical potential. *Nucl. Phys. B* **1999**, *558*, 327–346. [CrossRef]

57. Alles, B.; D'Elia, M.; Giacomo, A.D. Topological susceptibility at zero and finite T in SU(3) Yang-Mills theory. *Nucl. Phys. B* **1997**, *494*, 281–292; Erratum in **2004**, *679*, 397–399. [CrossRef]
58. Alles, B.; D'Elia, M.; Lombardo, M.P. Behaviour of the topological susceptibility in two colour QCD across the finite density transition. *Nucl. Phys. B* **2006**, *752*, 124–139. [CrossRef]
59. Lombardo, M.; Paciello, M.L.; Petrarca, S.; Taglienti, B. Glueballs and the superfluid phase of Two-Color QCD. *Eur. Phys. J. C* **2008**, *58*, 69–81. [CrossRef]
60. Hands, S.; Kim, S.; Skullerud, J. A Quarkyonic Phase in Dense Two Color Matter? *Phys. Rev. D* **2010**, *81*, 091502. [CrossRef]
61. Hands, S.; Kenny, P. Topological Fluctuations in Dense Matter with Two Colors. *Phys. Lett. B* **2011**, *701*, 373–377. [CrossRef]
62. Hands, S.; Kenny, P.; Kim, S.; Skullerud, J. Lattice Study of Dense Matter with Two Colors and Four Flavors. *Eur. Phys. J. A* **2011**, *47*, 60. [CrossRef]
63. Astrakhantsev, N.Y.; Bornyakov, V.G.; Braguta, V.V.; Ilgenfritz, E.M.; Kotov, A.Y.; Nikolaev, A.A.; Rothkopf, A. Lattice study of static quark-antiquark interactions in dense quark matter. *J. High Energy Phys.* **2019**, *2019*, 171. [CrossRef]
64. Iida, K.; Itou, E.; Lee, T. Two-colour QCD phases and the topology at low temperature and high density. *J. High Energy Phys.* **2020**, *2020*, 181. [CrossRef]
65. Boz, T.; Giudice, P.; Hands, S.; Skullerud, J. Dense two-color QCD towards continuum and chiral limits. *Phys. Rev. D* **2020**, *101*, 074506. [CrossRef]
66. Appelquist, T.; Ratnaweera, A.; Terning, J.; Wijewardhana, L.C.R. The Phase structure of an SU(N) gauge theory with N(f) flavors. *Phys. Rev. D* **1998**, *58*, 105017. [CrossRef]
67. Appelquist, T.; Sannino, F. The Physical spectrum of conformal SU(N) gauge theories. *Phys. Rev. D* **1999**, *59*, 067702. [CrossRef]
68. Orlando, D.; Reffert, S.; Sannino, F. Charging the Conformal Window. *Phys. Rev. D* **2021**, *103*, 105026. [CrossRef]
69. Brandt, B.B.; Endrodi, G. QCD phase diagram with isospin chemical potential. *PoS LATTICE* **2016**, *2016*, 039.
70. Bornyakov, V.G.; Nikolaev, A.A.; Rogalyov, R.N.; Terentev, A.S. Gluon Propagators in $2+1$ Lattice QCD with Nonzero Isospin Chemical Potential. *arXiv* **2021**, arXiv:2102.07821.
71. Bali, G.S.; Endrodi, G.; Gavai, R.V.; Mathur, N. Probing the nature of phases across the phase transition at finite isospin chemical potential. *arXiv* **2016**, arXiv:1610.00233.
72. Endrődi, G. Magnetic structure of isospin-asymmetric qcd matter in neutron stars. *Phys. Rev.* **2014**, *90*, 094501. [CrossRef]
73. Braguta, V.V.; Goy, V.A.; Ilgenfritz, E.M.; Kotov, A.Y.; Molochkov, A.V.; Muller-Preussker, M.; Petersson, B. Two-Color QCD with Non-zero Chiral Chemical Potential. *J. High Energy Phys.* **2015**, *2015*, 094. [CrossRef]
74. Espriu, D.; Nicola, A.G.; Vioque-Rodríguez, A. Chiral perturbation theory for nonzero chiral imbalance. *J. High Energy Phys.* **2020**, *2020*, 062. [CrossRef]